Broadband Single-Mode Hollow Substrate Integrated Waveguide with Photonic Crystal Sidewalls for Multilayer System-in-Package Applications

Binbin Hong, Yanbing Qiu, Lei Sun, and Guo Ping Wang
Institute of Microscale Optoelectronics
Shenzhen University
Shenzhen, China
b.hong@szu.edu.cn, iybqiu@gmail.com, lsun@szu.edu.cn, gpwang@szu.edu.cn

Nonchanutt Chudpooti
Research Center of Innovation Digital and Electromagnetic Technology (iDEMT), Department of Industrial Physics and Medical Instrumentation, Faculty of Applied Science
King Mongkut's University of Technology North Bangkok
Bangkok, Thailand
nonchanutt.c@sci.kmutnb.ac.th

John E. Cunningham, Ian D. Robertson and Nutapong Somjit
School of Electronic and Electrical Engineering
University of Leeds
Leeds, United Kingdom
j.e.cuningham@leeds.ac.uk, i.d.robertson@leeds.ac.uk, n.somjit@leeds.ac.uk

Abstract—We numerically and experimentally demonstrate a broadband single-mode hollow substrate integrated waveguide using one-dimensional photonic crystal as sidewalls in place of metallic via holes. By avoiding the vertical metallic walls, the waveguide can be easily fabricated as a photonic crystal structure on a single planar substrate sandwiched between two parallel metal plates. Such a hybrid flat waveguide can tightly confine the millimeter and terahertz waves in the low-loss air core. With the aid of the photonic crystal sidewalls, high-order competing modes in the waveguide are substantially suppressed based on the so-called modal-filtering effect, allowing the waveguide to be operated in a single-HE_{01}-mode pattern over an octave bandwidth. Benefiting from the less use of metallic walls, the propagation loss of the proposed hybrid waveguide can be less than that of the classic hollow metallic rectangular waveguide at millimeter-wave and terahertz frequencies according to our numerical simulation. A proof-of-concept experimental demonstration operating between 20 to 45 GHz is presented verifying the properties and the advantages of the proposed waveguide. This works offers a promising candidate for an octave-bandwidth single-mode transmission line for millimeter-wave and THz multilayer system-in-package applications.

Keywords—hollow substrate integrated waveguide, photonic crystal, modal-filtering effect.

I. INTRODUCTION

The characteristic scales of terahertz (THz) waves (0.3~3 THz≡0.1~1 mm≡10~100 cm-1≡1.24~12.4 meV) in the dimensions of time, space and photon energy are closely related to many unique phenomena in nature. Therefore, in recent years, it has attracted widespread attention from all sectors of society. THz technology has a wide range of application prospects, such as public safety, astronomical observation, fusion plasma diagnosis, medical and agricultural imaging, wireless communication, and chemical and biological species discrimination, etc. [1-3]

Historically, this section of the spectrum is also called the "THz gap", because this section of the spectrum is located in the blank area between electronics and optical technology, making it difficult to generate THz waves with artificial radiation sources. This has also led to the THz band becoming the last field in the electromagnetic spectrum that has not been fully explored and fully utilized. When traditional electronics and optical radiation sources approach the THz frequency band from their respective fields, their output power generally shows a rapid decline [4]. At the same time, the transmission loss of planar waveguides (such as microstrip lines, coplanar waveguides, strip lines, dielectric integrated waveguides, rectangular metal and rectangular dielectric waveguides, etc.) used in traditional integrated circuits is on the rise [5, 6]. The contradictory relationship between low output power of THz source and high waveguide loss is one of the key bottlenecks restricting the development and application of THz integrated circuits.

Reducing the transmission loss of the THz waveguide is one of the key methods to effectively solve the above-mentioned problem. In recent years, THz low-loss waveguides have become a hot research field. The methods used include both electronic methods, optical methods, and a combination of the two. The transmission loss of the traditional planar transmission line increases with the increase of the operating frequency, and it is very significant around 1 THz, which is much higher than the loss of the rectangular metal waveguide in the same frequency band [6]. The substrate integrated waveguide supports ultra-wideband transmission through mode selection, and the loss at 0.5 THz is 3.5 dB/cm, which is more than an order of magnitude lower than the loss of a microstrip line in the same frequency band [7]. However, when the substrate integrated waveguide works in the higher frequency THz band, its transmission loss will continue to increase, and it faces the problem of too small metal vias which is difficult to process using industrial PCB

fabrication techniques. When low-loss dielectric materials (such as high-resistivity silicon) are used as the main part of the material, the transmission losses of rectangular dielectric waveguides and photonic crystal waveguides in the THz band are very low [8]. However, the operating bandwidth supported by these two types of waveguides is relatively narrow, and they are susceptible to the influence of the dielectric properties of the surrounding space (such as the superstrate and the substrate), which is not conducive to the application in multilayer integrated circuits. Due to its advantages of simple design, low transmission loss, and stable operation, hollow metallic rectangular waveguides (HMRWs) are mainly used in devices and equipment with high performance requirements, such as spaceborne THz detectors, frequency extender of high-frequency vector networks analyzer, etc. However, in the band of 1 THz and above, HMRWs have problems such as difficulty in processing, high cost, and difficulty in integration. Therefore, so far, it is of great interest to develop low-loss THz waveguide that are easy to process, integrate, and stack for multilayer system-in-package applications.

In this paper, we show that millimeter and THz waves can be tightly confined in the air core of a hybrid waveguide that is essentially a hollow rectangular waveguide with one-dimensional photonic crystal instead of vertical side walls. By avoiding the vertical walls, the waveguide can be fabricated as a photonic crystal structure on a single planar substrate sandwiched between two parallel ground planes, with no metalized via holes. It is, in essence, a flat form of the well-known Bragg fiber [9] that can be realized on a single substrate and so we call it a Substrate Integrated Bragg Waveguide (SIBW). According to our theoretical analysis, the proposed waveguide operates in the fundamental HE_{10} mode while suppressing the high-order competing modes using a modal-filtering effect, which allows the waveguide to operate in single-mode fashion over more than one octave. A proof-of-concept millimeter-wave (mmW) waveguide was designed and tested in order to verify the transmission properties of the proposed structure. The proposed novel waveguide could offer a step towards a hybrid transmission-line medium that can be used in a variety of functional components for multilayer integration and broadband applications.

II. PRINCIPLE

Fig. 1(a) shows the trimetric view of the proposed SIBW with the key design parameters indicated. The top and bottom layers are a pair of parallel metal plates, and the middle layer is an air-core line-defect 1D photonic crystal Bragg reflector structure. The Bragg reflector consists of periodically alternating layers of high- and low-refractive-index materials. Air is chosen as the low-refractive-index material for its low refractive index and low loss. Another material that forms the Bragg reflector is desired to be high refractive index and low loss, to create a large photonic bandgap and reduce the material absorption loss. High-resistivity silicon is one of the most commonly used materials which has high refractive index and low absorption loss in the THz frequency range, and thus it is chosen as the high-refractive-index component of the photonic crystal in our theoretical analysis. The high-resistivity silicon is dispersionless, and the real part of its complex refractive index is 3.4175 ± 0.00005 between 0.5 and 4.5 THz. The fundamental mode of the proposed SIBW is a vertically polarized TE_{10} mode. The height of the SIBW, h, is adjustable, but it will slightly affect the performance, and will
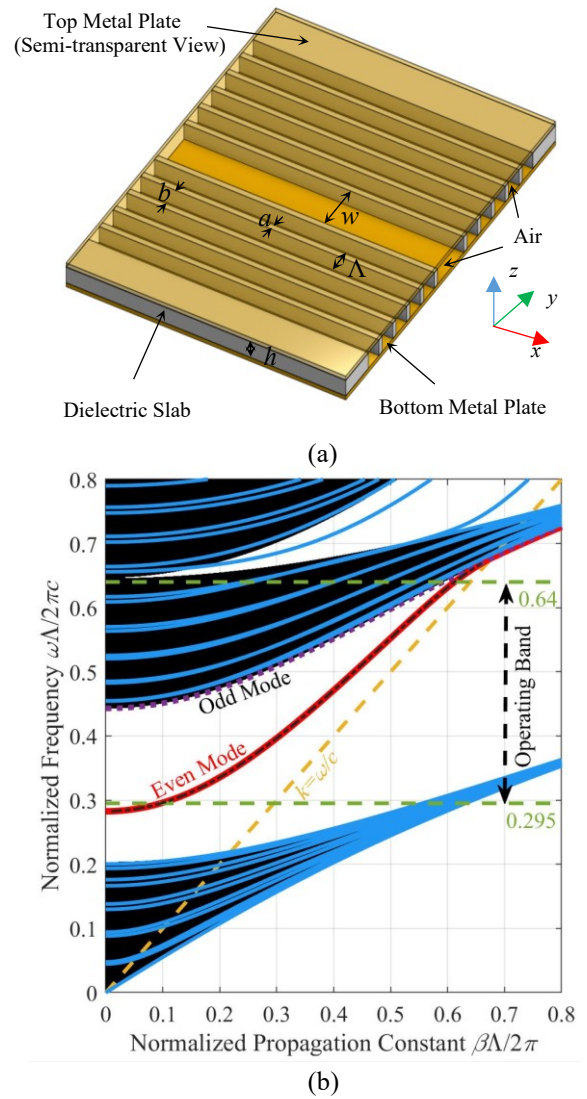

(a)

(b)

Fig.1. (a) Schematic diagram of the proposed SIBW with the key design parameters indicated. $\Lambda = a + b$ is the period of the photonic crystal structure. $w = 1.89\Lambda$ is the width of the line defect in the core region. $h \leq w/2$ is the thickness of the dielectric slab. (b) Projected bandgap diagram and dispersion curves for the vertically polarized modes in the SIBW. Here, the dielectric slab is silicon, $a = 0.2276\Lambda$, and $b = 0.7724\Lambda$. The orange dashed line is the light line. The green dashed lines indicate the operating band which is wider than one octave. The black region is the bandpass region for the 1D photonic crystal in which the electromagnetic wave can pass through the periodic structure and leak out. The white region above the light line is the bandgap. The red solid line and the purple dotted line represents the dispersion curves for the fundamental HE_{10} mode and the second-order competing HE_{20} mode, respectively. The blue curves overlaid upon the black region are cladding modes or lossy defect modes whose electric field are mainly distributed in the bulk crystal.

introduce high order modes if the value of is too large. In this paper, a SIBW with a thin dielectric slab, namely, $h < w/2$, is considered. Since the electric field of the TE_{10} mode is uniform along the z-axis, h does not contribute to the dispersion relation. Therefore, the dispersion relation problem can be simplified into a 2D problem in the x-y plane assuming the third dimension is infinite and uniform, and it represents the eigenvalues for the vertically (z-axis) linearly polarized modes confined in the core of the Bragg reflector waveguide.

Dispersion curves for vertically (z-axis) linearly polarized modes in the line-defect Bragg reflector waveguide overlaid upon the projected bandgap diagram are shown in Fig. 1(b).
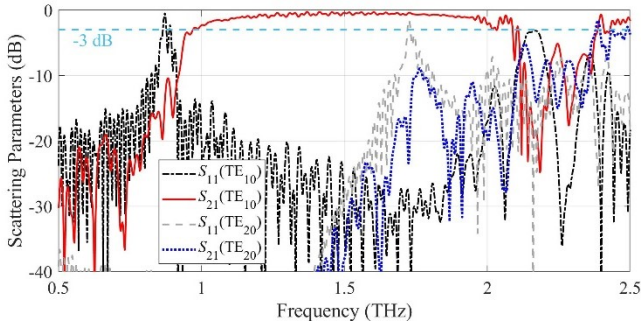
Fig. 2. Scattering Parameters for SIBW when different modes are excited in the HMRW. The length of the SIBW is 3 mm.

For the sake of plotting the projected bandgap diagram with a dimensionless property in Fig. 1(b), the longitudinal propagation constant β is scaled with $2\pi/\Lambda$. The value of $\beta\Lambda/2\pi$ is not restricted between -0.5 and 0.5, as the structure has continuous translational symmetry in the longitudinal direction. Similar to photonic crystal fiber, a complete bandgap is not necessary for the proposed waveguide. Because of the translational symmetry, the propagation constant β is conserved, and it is therefore still useful to have bandgap over some finite range of β. The dispersion curves are numerically calculated using the open-source MIT Photonic-Bands (MPB) package and commercial finite element software COMSOL, while the photonic bandgap is calculated separately and analytically according to Bloch's theorem [10]. MPB simulates the above-mentioned 2D simplified structure assuming infinitely extending dielectric lamellae in the z-direction, while COMSOL simulates the 3D full structure taking into account the top and bottom metal plates. From Fig. 1(b), we can see that the dispersion curves of the fundamental guide even mode calculated using both methods are coincident with each other. Thus, the simplified 2D model presents the problem related to vertically polarized modes very well. The frequency range between the two horizontal green dashed lines in Fig. 1(b) gives the operating band of this design. The selected operating band gives a ratio bandwidth of $\omega_n^h/\omega_n^l \approx 2.17$, which is wider than one octave.

III. SIMULATION

By choosing $\Lambda = 93.1\ \mu m$, the operating band of the above-mentioned SIBW is settled around the frequency range of $(\omega_n^l c/\Lambda,\ \omega_n^h c/\Lambda) = (0.95\ \text{THz}, 2.06\ \text{THz})$. In the following simulations, a representative surface roughness equal to 1.5 times of the skin depth of copper is considered. Here, the skin depth of copper is calculated at the central frequency point under the condition of room temperature (293 K) and DC conductivity of 5.967×10^7 S/m. The built-in tabulated impedance model of CST is used to obtain the declined dispersive surface conductivity of copper. Wave propagation in the SIBW was studied using commercial package CST Microwave Studio time-domain solver. A HMRW, whose width (176 μm) and height (88 μm) are equal to those of the defect core of the SIBW, was chosen to feed the SIBW. The single-mode operating frequency range of the HMRW is between 0.85 THz and 1.70 THz, so at frequencies above 1.70 THz, high order modes, such as TE_{20}, TE_{01}, etc., can be excited by the HMRW.

The scattering parameters for the SIBW when different modes in the HMRW are excited are shown in Fig. 2. Here, scattering parameters are defined based on voltage ratios of the incident and reflected voltage waves and are in decibel

form. From the S_{21} frequency response, when TE_{10} mode is excited, we observe that a transmission window wider than an octave centered at about 1.5 THz is supported in the SIBW. The S_{11} response when the TE_{10} mode is excited indicates that the impedance mismatch between the TE_{10} mode in the HMRW and the HE_{10} mode in the SIBW is low, since the reflection coefficient is basically below -15 dB from 1 to 2 THz. When the second-order TE_{20} mode is excited in the HMRW at around 1.7 THz, the S21 rises but it is still below -9 dB owing to the modal-filtering effect, and therefore the high-order mode is suppressed. Under the high-order mode (TE_{20}) excitation condition, the S_{11} is high at around 1.7 THz which means the impedance mismatch is large at the waveguide transition, and at around 2 THz, both S_{11} and S_{21} are relatively small indicating that the second-order mode is leaky in the SIBW because the electromagnetic field is neither reflected nor transmitted. In addition to the TE_{20} mode, other high-order modes operate at higher frequencies, which is beyond the frequency range of interest from 1 to 2 THz.

IV. SCALED MEASUREMENT

To facilitate the fabrication and measurement, a proof-of-concept experimental demonstration of SIBW was performed at millimeter-wave frequencies (ranging from 20 to 45 GHz). Two SIBW samples with different lengths and fed by microstrip and coaxial launchers were fabricated and tested, as shown in Fig. 3. The dielectric material used for the SIBW is Rogers RO3010, which has a dielectric constant of 10.2 and loss tangent of 0.0022 over the frequency range from 8 to 40 GHz. The substrate for the microstrip is double-sided copper-clad Rogers RT/Duroid 5880LZ ($\varepsilon_r = 2$). The thicknesses of the dielectric and copper claddings of both substrates were 0.635 mm and 17.5 μm, respectively. The design principles are the same as those discussed in the principle section. The reason why we use the Rogers RO3010 substrate rather than high-resistivity silicon is that the PCB board is compatible with standard PCB fabrication techniques. The similarities between the RO3010 and the high-resistivity silicon are that they both have relatively high dielectric constant and low absorption loss, which are desirable for constructing the designed photonic crystal structure.

A two-tier calibration technique was used to characterize the SIBW. The first-tier SOLT calibration was performed using a 2.4mm mechanical calibration kit to place the reference planes to the input interface of the end launch connectors. A second-tier calibration used multiline calibration to de-embed using the complex propagation
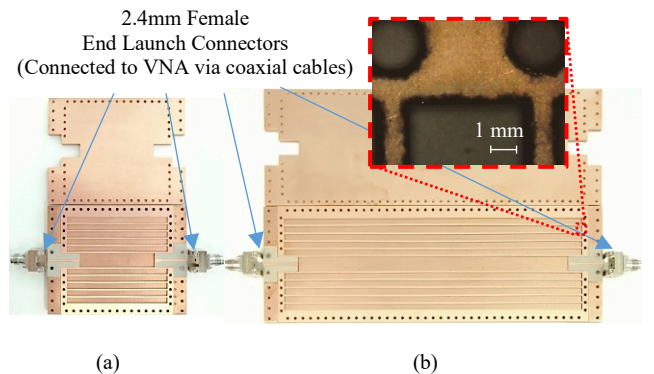

(a)   (b)

Fig.3. (a) Short SIBW with the length between the two microstrip lines $l = 46.54$ mm. (b) Long SIBW with $l = 150.56$ mm. The inserted picture in (c) shows the zoomed view of the photonic crystal structure. In the design, $a = 1$ mm, $b = 3.28$ mm, $w = 8.14$ mm, and $h = 0.671$ mm
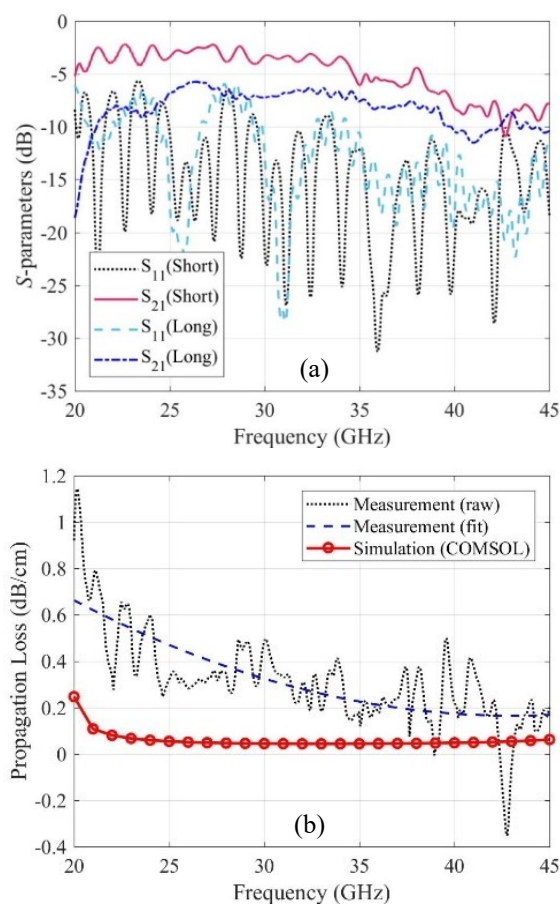
Fig.4. Characterization of the SIBW. (a) Measured S-parameters of the two SIBW samples. One percentage moving window smoothing, a built-in feature of the VNA, is applied to reduce the very high-frequency ripples due to minor impedance mismatches at fabrication imperfections. (b) Simulated and measured propagation loss. Second-order polynomial curve fitting is applied to fit the measured propagation loss.

constant of the SIBW. The two SIBW samples were tested using a vector network analyzer and the scattering parameters are shown in Fig. 4(a). A two-tier calibration technique was used to characterize the SIBW. The first-tier SOLT calibration was performed using a 2.4mm mechanical calibration kit to place the reference planes to the input interface of the end launch connectors. A second-tier calibration used multiline calibration to de-embed using the complex propagation constant of the SIBW. The two SIBW samples were tested using a vector network analyzer and the scattering parameters are shown in Fig. 4(a). The reflection coefficients (S_{11}) of the two SIBWs are lower than -6 dB (<25%) over the frequency of interest between 20 and 45 GHz, which means that a significant amount of the power was fed into the SIBWs. Besides, the magnitude of the S_{11} parameters for the short and long SIBWs are at the same level, which means that the repeatability of the microstrip to SIBW transitions for both SIBWs are acceptable for multiline calibration. The transmission coefficients (S_{21}) for both SIBWs show wideband transmission windows ranging from 20 to 45 GHz which are wider than one octave.

The simulated and measured propagation losses of the SIBW are shown in Fig. 4(b). In general, the measured and fitted simulated results follow similar trends, namely, the propagation losses decrease firstly with increasing frequency and then increases after reaching a minimum. On average, the measured propagation loss of the fabricated SIBW is less than 0.66 dB/cm (compared with 0.25 dB/cm simulated) over the frequency range from 20 to 45 GHz, which is wider than one

octave. The measured loss is observed to be greater than the simulated results, which may due to several factors that increase the loss such as surface roughness, oxidation of the copper layer, residual burnt dielectric material, and fabrication or assembly imperfections.

V. CONCLUSION

This paper presents a substrate integrated Bragg waveguide that can operate in single-HE_{10}-mode over more than one octave. First, we theoretically investigated the SIBW between 1 to 2 THz, and the propagation loss of the proposed SIBW is found to be even lower than that of a classic HMRW, benefiting from the reduction of Ohmic loss. To facilitate the fabrication and measurement, we performed a proof-of-concept experimental demonstration at mmW frequencies ranging from 20 to 45 GHz to verify the guidance properties of the proposed SIBW, such as the operating bandwidth, operating mode, and propagation loss, with consistency between the theoretical analyses and the experimental measurements being observed. Showing many advantages over conventional THz planar waveguides, the proposed SIBW is a promising hollow hybrid transmission line for broadband mmW and THz systems using functional components or multilayer multichip module technology.

REFERENCES

[1] P. U. Jepsen, D. G. Cooke, and M. Koch, "Terahertz spectroscopy and imaging–Modern techniques and applications," Laser Photonics Rev., 5(1), 124-166 (2011).

[2] S. S. Dhillon, M. S. Vitiello, E. H. Linfield, A. G. Davis, M. C. Hoffmann, J. Booske, … and M. B. Johnston, "The 2017 terahertz science and technology roadmap," J. Phys. D Appl. Phys., 50(4), 043001 (2017).

[3] I. Robertson, N. Somjit, and M. Chongcheawchamnan, Microwave and millimetre-wave design for wireless communications, (John Wiley & Sons, 2016).

[4] Yazgan, L. Jofre, J. Romeu, "The state of art of terahertz sources: A communication perspective at a glance," In 2017 40th International Conference on Telecommunications and Signal Processing (TSP), Barcelona: IEEE, 810-816 (2017).

[5] D. R. Grischkowsky, "Optoelectronic characterization of transmission lines and waveguides by terahertz time-domain spectroscopy," IEEE J. Sel. Top. Quantum Electron., 6(6), 1122-1135 (2000).

[6] J. Cabello-Sánchez, H. Rodilla, V. Drakinskiy, and J. Stake, "Transmission Loss in Coplanar Waveguide and Planar Goubau Line between 0.75 THz and 1.1 THz," In 2018 43rd International Conference on Infrared, Millimeter, and Terahertz Waves (IRMMW-THz) (pp. 1-2). IEEE (2018).

[7] F. Fesharaki, T. Djerafi, M. Chaker, and K. Wu, "Guided-wave properties of mode-selective transmission line," IEEE Access, 6, 5379-5392 (2017).

[8] A. Malekabadi, S. A. Charlebois, D. Deslandes, and F. Boone, "High-resistivity silicon dielectric ribbon waveguide for single-mode low-loss propagation at F/G-bands," IEEE Trans. Terahertz Sci. Technol., 4(4), 447-453 (2014).

[9] P. Yeh, A. Yariv, and E. Marom, "Theory of Bragg fiber," J. Opt. Soc. Am. A., 68(9), 1196-1201 (1978).

[10] P. Yeh, A. Yariv, and C.-S. Hong, "Electromagnetic propagation in periodic stratified media. I. General theory," J. Opt. Soc. Am., 67(4), 423-438 (1977).